Journal of Applied Science and Engineering, Vol. 17, No. 3, pp. 223–230 (2014) *DOI: 10.6180/jase.2014.17.3.02*

On Deriving Surface Tension Force in MEMS

Lung-Jieh Yang*, Kuan-Chun Liu and Wei-Chung Lin

Department of Mechanical & Electromechanical Engineering, Tamkang University, Tamsui, Taiwan 251, R.O.C.

Abstract

This paper presents the comparison between the force balance method and the surface energy method in deriving surface tension forces of some microelectromechanical systems (MEMS) problems. For studying the force balance of the capillary rise in the wick structure of heat pipes or heat spreaders, not only the surface tension at the three-phase interfaces but also the free surfaces should be carefully considered. Meanwhile the intrinsic scalar quantity of surface energy method proves its systematic feature without too much physical insight into the surface tension issues. Finally the authors used the surface energy method to study the capillary stiction of a cantilever beam during its drying process. A surface tension-driven cantilever array using for flapping micro-air-vehicles (FMAVs) is exemplified to justify the theoretical prediction in a static manner.

***Key Words*:** Surface Tension, Free Surface, Cantilever, Stiction

1. Introduction

The capillary phenomenon was firstly investigated in the early stage of the 19th century [1–3]. Since microfluidic sensors and actuators are involved, the kinematics of the capillary meniscus and the related surface tension forces are those of microscopic dimensions in the classical mechanics which are still very important. Although the contact angle measurements and the liquid filling experiments [4–6] have been employed for decades to study the capillary phenomenon, a systematic theoretical analysis is not often found [5]. It's the motivation of this paper to review the surface energy method for realizing the kinematics of the capillary meniscus in many micro engineering problems such as the surface stiction in surface micromachinings [7], capillary heat pipes [8], surface tension-driven devices [5,9], and so on.

There are at least two general ways to evaluate the total surface tension force applied on the fluidic column in a microchannel or a microgap. Herein, one is the force balance method, and the other is the surface energy method. For the former, people look at the liquid/solid/air interface (or the meniscus) and summarize the surface tension force by multiplying the difference ($\gamma_{sa} - \gamma_{sl}$) with the perimeter length of the meniscus contour. For the latter, the total surface tension force along a specific direction can be deduced from differentiating the surface energy of the whole liquid system with respect to the spatial coordinate of that specific direction [7].

In this paper, the authors firstly take the liquid column rise in a rectangular microchannel as an example to demonstrate the advantage of the surface energy method over the force balance method [8]. Thereafter, the surface stiction in the surface micromachining and some surface tension-driven microelectromechanical systems (MEMS) devices are discussed by this systematic energy approach.

2. Liquid rise in a Rectangular Closed Microchannel

Consider a vertical capillary with a rectangular cross section in Figure 1. The dimension is denoted as w(width) × h(thickness) × L(length). The liquid column

*Corresponding author. E-mail: Ljyang@mail.tku.edu.tw

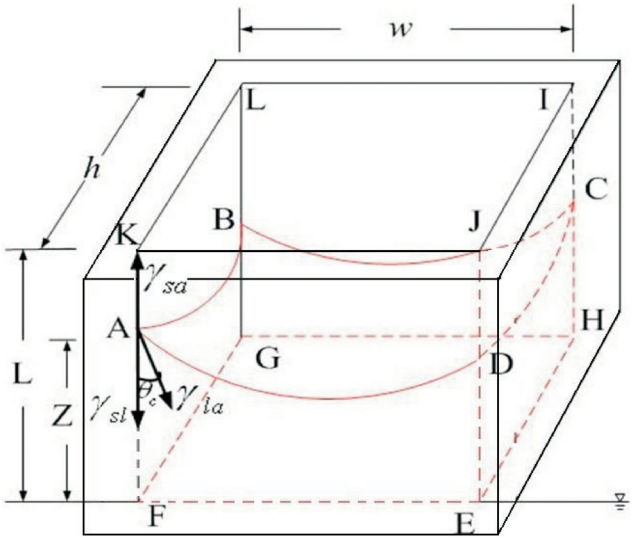

Figure 1. The capillary rise in a closed microchannel.

rise from the water horizon is with the height of Z which is a variable here. Three surface tension forces (per unit perimeter length) include γ_{la}, γ_{sa}, γ_{sl} at the three-phase (liquid/solid/air) interface or the meniscus position satisfying Young's law [1–3]:

$$\gamma_{sa} - \gamma_{sl} = \gamma_{la}\cos\theta_c \tag{1}$$

where θ_c is the contact angle.

2.1 Force Balance Method

By the force balance method, the gravitation of the arisen liquid column is equal to the net surface tension force. i.e., the term with $(\gamma_{sa} - \gamma_{sl})$ multiplied by the full perimeter length of the rectangular meniscus contour $2(h + w)$. The authors ignore the complicated curve shape of the meniscus and simplify it as a flat surface.

$$(\gamma_{sa} - \gamma_{sl})2(h + w) = \rho g w h Z \tag{2}$$

or

$$Z = \frac{2(h+w)\gamma_{la}\cos\theta_c}{\rho g w h} \tag{3}$$

where ρ and g denote the density of the liquid and the gravitation, respectively. This derived liquid column rise Z of Equation (3) will be shown identical to the one from the surface energy method shown as below.

2.2 Surface Energy Method

The total surface energy of the capillary channels for heat pipes with water rise is composed of four parts in Figure 1. The 1st part is the vacant wall area $2(L - Z)$ $(h + w)$ multiplied by γ_{sa}. The 2nd part is the wetting wall area $2Z(h + w)$ multiplied by γ_{sl}. The 3rd part is the surface of the capillary meniscus area approximated by wh and multiplied by γ_{la}. The 4th part is the surface energy E_0 stored in the huge liquid reservoir. E_0 hardly changes due to the very small amount of liquid filling into the capillary [5,10].

Therefore the total surface energy of the capillary channel in Figure 1 is expressed as below.

$$E_S = E_0 + 2(L - Z)(h + w)\gamma_{sa} + 2Z(h + w)\gamma_{sl} + wh\gamma_{la} \tag{4}$$

Taking the derivative of Equation (4) with respect to Z, the authors obtain the equivalent force F_s applied on the liquid column along the Z-direction, and it is equal to the gravitation.

$$F_S = -\frac{dE_s}{dZ} = 2(h+w)(\gamma_{sa} - \gamma_{sl}) = \rho g w h Z \tag{5}$$

Equation (5) is exactly equivalent to Equation (2). Herein, the force balance method and the surface energy method give the same expression of the capillary rise Z in Figure 1. Moreover, the force balance method seems more concise and more straightforward. However, the authors wonder whether these two methods would always generate the same results in other examples or not?

3. Liquid Rise in a Rectangular Open Groove

The authors change the configuration of microchannel filling from Figure 1 to Figure 2. The many micro grooves like the single one in Figure 2 are used as the wick structure of heat pipes or heat spreaders [8]. The authors would like to discuss the capillary rise Z again by the force balance method and the surface energy method respectively.

3.1 Force Balance Method

With the first glance, using the force balance method to analyze the issue of Figure 2, the authors evaluate the

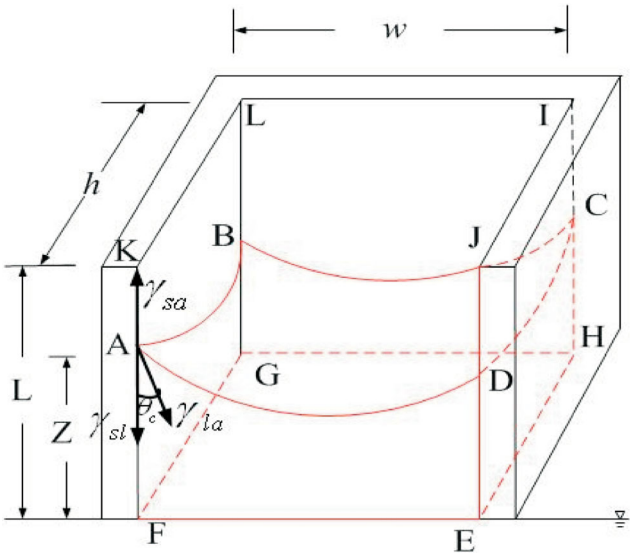

Figure 2. A single vertical capillary groove with a water rise.

surface tension difference ($\gamma_{sa} - \gamma_{sl}$) seems only multiplied by three sides rather than the full perimeter of the rectangular groove. In other words, ($2h + w$) at the three-phase interface are multiplied with ($\gamma_{sa} - \gamma_{sl}$) to counter balance the gravity of the liquid column rise Z.

$$(\gamma_{sa} - \gamma_{sl})(2h + w) = \rho g w h Z \tag{6}$$

or

$$Z = \frac{(2h + w)\gamma_{la} \cos\theta_c}{\rho g w h} \tag{7}$$

where $\gamma_{la} = 0.073$ N/m, $h = 430$ μm, $\theta_c = 33°$ [8].

But Equation (7) actually does not match the experimental data in Figure 3 very well. The data variations seem invariant with the groove width w. The force balance method at the first glance herein seems not get the good approximation and need further improvement. The reason is due to that the force contribution from the free surface has not been considered yet. Before showing the proper manipulation of the force method to this problem the authors would like to resort to the other way, the surface energy method at first.

3.2 Surface Energy Method

Regarding the total surface energy of Figure 2, the authors still have four parts to discuss. Firstly, the vacant wall area is ($L - Z$) ($2h + w$) and it's needed to be multiplied by γ_{sa}. Secondly, the wetting wall area is $Z(2h + w)$ needed to be multiplied by γ_{sl}. Thirdly, the curved capillary meniscus area is simplified as $w(h + Z)$ and multiplied by γ_{la}. Therefore,

$$E_S = E_0 + (L - Z)(2h + w)\gamma_{sa} + Z(2h + w)\gamma_{sl} + w(h + Z)\gamma_{la} \tag{8}$$

Taking the derivative of Equation (8) with respect to Z, the authors obtain the equivalent force F_s applied on the liquid column along the Z-direction, and it equals to the gravitation.

$$F_S = -\frac{dE_s}{dZ} = (2h + w)(\gamma_{sa} - \gamma_{sl}) - \gamma_{la} w = \rho g w h Z \tag{9}$$

or

$$Z = \frac{\gamma_{la}[(2h + w)\cos\theta_c - w]}{\rho g w h} \tag{10}$$

The theoretical prediction of Equation (10) is very close to the experimental data in Figure 4 [8], and proves the validity of the surface energy method which is better than the prediction of Equation (7) in the previous section.

The improper prediction of Equation (7) shows the wrong manipulation of the force balance method. In fact, tracing back the terms in Equations (8)–(10), the authors found that the capillary rise of Equation (7) lacks the contribution from the free surface ADEF in Figure 2. This force component of the free surface ADEF can be

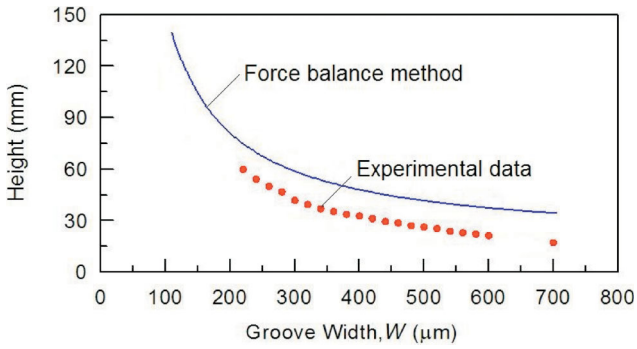

Figure 3. The experimental data of a capillary rise in the groove [8] compared with the result of force balance method.

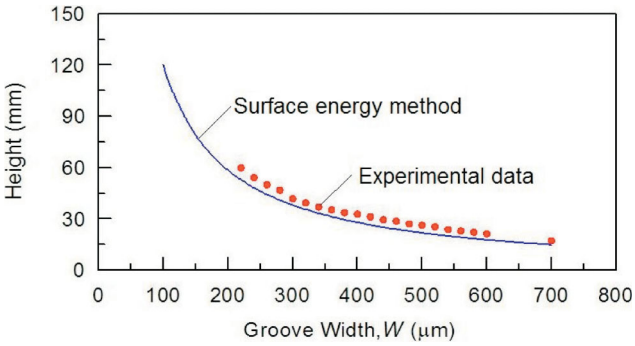

Figure 4. The experimental data of a capillary rise in the groove [8] compared with the result of surface energy method.

recognized by multiplying the liquid-air surface tension γ_{la} with the width w and with the opposite direction to other three forces at the groove walls. So the contribution $-\frac{\gamma_{la} w}{\rho g w h}$ invariant with the width w in Equation (10) is now well defined by this proper manipulation of force balance method. Restated, when water fills a groove in Figure 2, there will be four forces competing to move the meniscus - i) three forces at the groove walls and ii) one force on the free surface.

Summarizing the above two methods, the force balance method is a way easier to understand and more concise to use, but we need to be familiar with the surface force formulation both at the three-phase interfaces and on the free surfaces. The force direction should be also defined right. Regarding the systematic surface energy method, however, the intrinsic scalar quantity of surface energy does not need the judge of force direction with an exactly right physical insight. The only thing that the energy method needed to do is to summarize systematically all the surface energies subjected to their corresponding surface tensions (including γ_{la}, γ_{sa}, γ_{sl}). Then the authors promisingly obtain the resultant capillary force along any direction by differentiating its corresponding spatial coordinate in the following cases.

4. Surface Stiction of Micro Cantilevers

Micro cantilevers are usually assigned as the configuration for MEMS sensors and actuators. Using the surface micromachining to deposit the sacrificial and structural layers in sequence, people remove the sacrificial layer, dip in de-ionized (DI) water, and wait for drying the free standing devices. As the water above the free structure evaporates to some extent, the meniscus surface appears. The liquid between the cantilever and the substrate automatically has a tendency to minimize its surface. So a pull-down force is employed on the upper cantilever to deform vertically and may cause the stiction problem accordingly [10–12].

Regarding the cantilever involving the stiction issue in Figure 5, the residual liquid under the cantilever is defined as $x \times y \times h$, comparable to the vacant gap space $L \times W \times h$ of the cantilever.

There is no free surface in the problem of Figure 5. The surface tension forces $(\gamma_{sa} - \gamma_{sl})$ at the three-phase interfaces are along the horizontal direction rather than the vertical direction. So it's hard to figure out the surface tension force for pulling down the micro cantilever by the force balance method directly. Therefore the authors would like to use the surface energy method to derive the downward surface tension force herein. Similar to the surface energy method in the previous section, the authors summarize the total surface energy of Figure 5 as below.

$$\begin{aligned} U_S &= 2[A_{sa}\gamma_{sa} + A_{sl}\gamma_{sl}] + A_{la}\gamma_{la} \\ &= 2[(wL - xy)\gamma_{sa} + xy\gamma_{sl}] + (2x + y)h\gamma_{la} \\ &= 2[wL\gamma_{sa} + xy(\gamma_{sl} - \gamma_{sa})] + (2x + y)h\gamma_{la} \end{aligned} \tag{11}$$

where A_{sa} and A_{sl} are the areas of the solid-air and

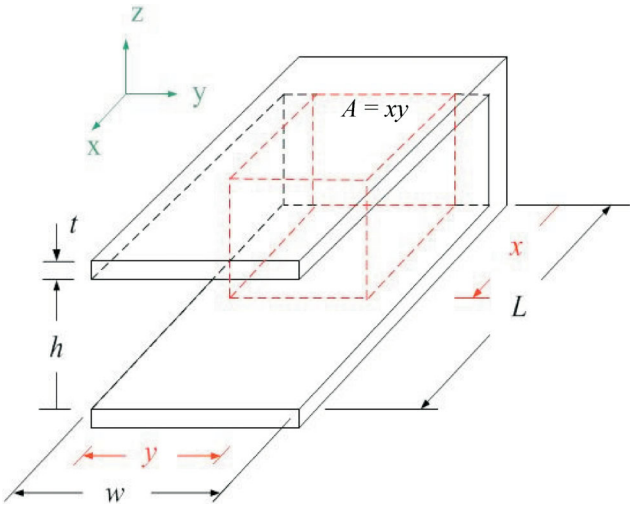

Figure 5. 3D configuration of a micro cantilever without deflection; h is much smaller than the other dimensions.

solid-liquid interfaces. The equation of the surface energy U_s neglects the complicated nature of the small liquid-air meniscus surface area [5,13] since this liquid-air area $(2x + y)h$ is much smaller than others.

Using Equation (1) and the constant volume of the liquid in the gap $V_0 = xyh$, the authors have the surface energy U_S expressed as below.

$$U_S = 2\left[wL\gamma_{sa} - \left(\frac{V_0}{h}\right)\gamma_{la}\cos\theta_c\right] \tag{12}$$

If the bottom plate or substrate remained fixed, a downward force must be applied to the cantilever to keep the equilibrium. This force is denoted as F_{cap}.

$$F_{cap} = -\left(\frac{dU_S}{dh}\right) = -\left(\frac{2V_0}{h^2}\right)\gamma_{la}\cos\theta_c = -\left(\frac{2A}{h}\right)\gamma_{la}\cos\theta_c; \quad A = xy \tag{13}$$

Divide Equation (13) with the solid-liquid surface $A = xy$ and give the capillary pressure or the so-called Laplace pressure exerted on the cantilever.

$$P_{Laplace} = \left|\frac{F_{cap}}{A}\right| = \frac{2\gamma_{la}\cos\theta_c}{h} \tag{14}$$

Equation (14) matches the expression of Laplace pressure mentioned in many prior literatures [2,4,5,7, 8,10–12]. This capillary force increases nonlinearly with the decreasing of the gap h. If we regard the maximum surface tension force F_{cap} as a uniform loading q along the cantilever beam, then q and the maximum downward deflection v_{max} at the cantilever tip predicted by elasticity theory [14] are as below.

$$q = \frac{\left|F_{cap,\max}\right|}{L} = \left(\frac{2w}{h}\right)\gamma_{la}\cos\theta_c \tag{15}$$

$$v_{\max} = \frac{qL^4}{8EI} = \frac{3\gamma_{la}\cos\theta_c}{E}\left(\frac{L^4}{ht^3}\right) \tag{16}$$

5. Experiment Verification of Micro Cantilevers

Similar to the small displacement of electrostatic actuators, the micro actuator using the capillary stiction force also has the disadvantage of small actuation stroke. This drawback can be remedied by the configuration of actuator array. The authors have ever developed a peacock-like comb-shaped actuator to have an obvious rotating stroke angle [9] and applied to the rudder of a flapping micro air vehicle (FMAV) [15]. The device is shown in Figure 6 and the structure material is the high aspect-ratio SU-8. The device fabrication is done by the ordinary UV-lithography. With more than 200 comb cantilevers, the total actuation angles are around 224°. The device dimensions are shown as below.

$L = 2{,}700\ \mu m$
$w = 80\ \mu m$
$t = 20\ \mu m$
$h = 20\ \mu m$

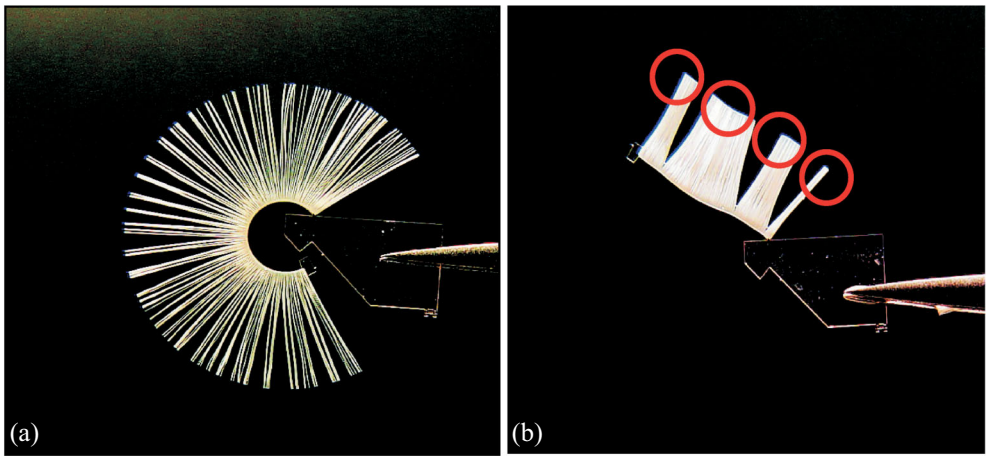

Figure 6. SU-8 peacock-like micro actuator of 6 mm size [9]; (a) without water; (b) with water.

$E = 4.4\ GPa$
$\gamma_{la} = 0.073\ N/m$
$\theta = 70°$

Substituting the above parameters into Equation (16), we have the maximum deflection at the cantilever tip as $v_{max} = 5654\ \mu m$. This unrealistic deflection much larger than the original gap $h = 20\ \mu m$ means that the cantilever beams are all stuck together subject to water wetting. The experimental photos are shown as Figure 6. While wetted with water, some local collapse of SU-8 cantilever tips show the permanent stiction even when water dries out in Figure 6(a). Moreover, the several stuck places marked with circles in Figure 6(b) are similar to the elastocapillary phenomena mentioned in Bico's work [16].

Additionally, the authors changed the structure material of the surface tension-driven actuator from SU-8 resist to stainless steel (SUS-304) foil [15]. The operations of this steel-based actuator are depicted in Figure 7. The dimension parameters and material property are shown as below.

$L = 3{,}000\ \mu m$
$w = 40\ \mu m$
$t = 50\ \mu m$
$h = 50\ \mu m$
$E = 200\ GPa$
$\gamma_{la} = 0.073\ N/m$
$\theta = 70°$

Substituting the above parameters into Equation (16), we have the maximum deflection at the cantilever tip as $v_{max} = 4.85\ \mu m$. This small deflection which is much smaller than the original gap $h = 50\ \mu m$ means that the cantilever beams are not stuck together subject to water wetting. Even referring to several small actuation angles of the steel-based bionic actuator corresponding to different wetting surface conditions in Figure 7, the non-stiction of this more stiffened device is verified preliminarily by the static model of Equation (16).

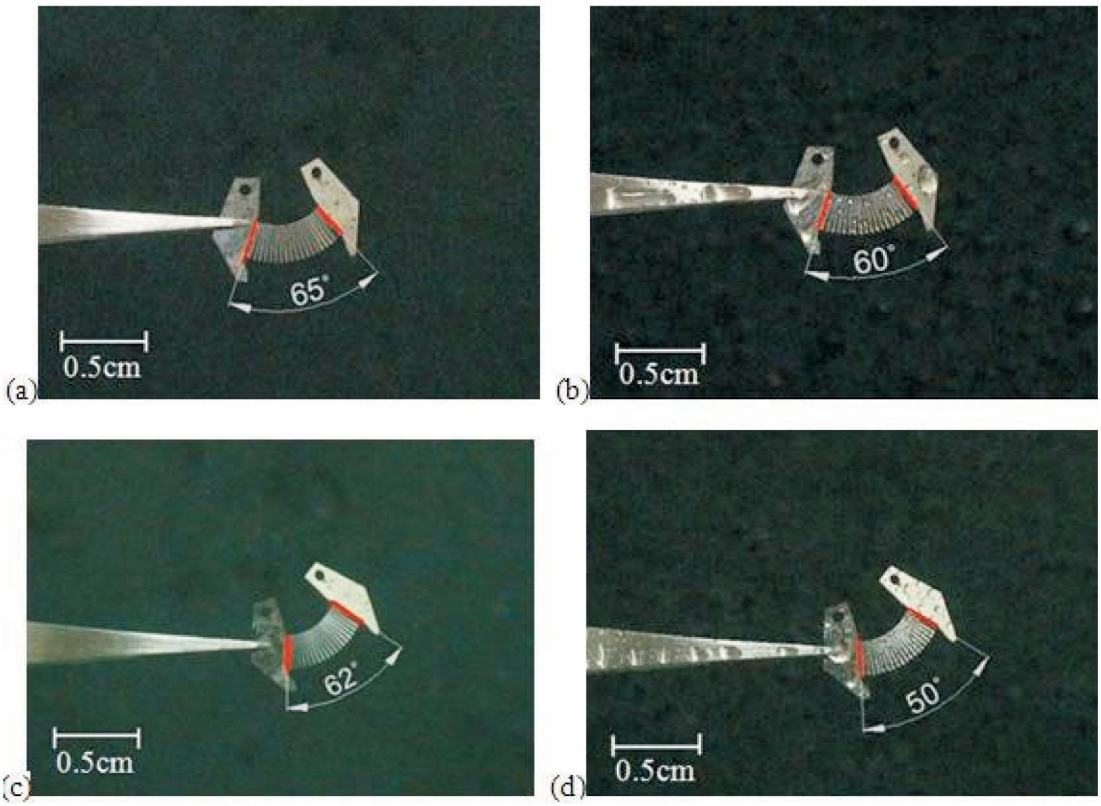

Figure 7. Angle changing of the steel-based bionic actuator due to the water surface tension: (a) steel actuator without water; (b) steel actuator with water; (c) parylene-coated steel actuator without water; (d) parylene-coated steel actuator with water [15].

Equation (16) is just a static model for predicting the deflection of a micro cantilever caused by surface tension force. If this static deflection v_{max} is much less than the original gap h between the cantilever and the ground base, no surface stiction is supposed to happen. However, the authors have not taken the nonlinear effect into account in Equation (16). In other words, the gap h in Equation (16) is actually not a constant but varied with v_{max} mutually. The exact deflection behavior or even the stiction condition should be resorted to the more sophisticated stability analysis in the future.

6. Conclusions

With the surface tension force derived by the surface energy method summarized in this paper, the author systematically predict the surface tension-driven deflection of a micro cantilever during its drying process. A peacock-like micro actuator using cantilever array as the rudder for a FMAV was demonstrated as an example to verify the theoretical prediction. The micro cantilever made by SU-8 resist was stuck after water drying, but the device made by stainless steel foil can withstand the capillary pull down force. Therefore this elastocapillary static model without the consideration of stability is preliminarily confirmed herein.

References

[1] de Genes, P. G., "Wetting: Statics and Dynamics," *Rev. Mod. Phys*., Vol. 57, pp. 827–890 (1985). doi: 10.1103/RevModPhys.57.827

[2] Israelachvili, J. N., *Intermolecular and Surface Forces*, Academic, London, p. 120 (1985).

[3] Madou, M., *Fundamentals of Microfabrication*, 2nd Ed., CRC, New York, p. 584 (2002).

[4] Sobolev, V. D., Churaev, N. V., Velarde, M. G. and Zorin, Z. M., "Surface Tension and Dynamic Contact Angle of Water in Thin Quartz Capillaries," *J. Colloid Interface Sci.*, Vol. 222, No. 1, pp. 51–54 (2000). doi: 10.1006/jcis.1999.6597

[5] Yang, L. J., Yao, T. J. and Tai, Y. C., "The Marching Velocity of the Capillary Meniscus in a Microchannel," *J. Micromech. Microeng*., Vol. 14, No. 2, pp. 220–225 (2004). doi: 10.1088/0960-1317/14/2/008

[6] Chan, W. K. and Yang, C., "Surface-Tension-Driven Liquid-Liquid Displacement in a Capillary," *J. Micromech. Microeng*., Vol. 15, No. 9, pp. 1722–1728 (2005). doi: 10.1088/0960-1317/15/9/014

[7] Tas, N., Sonnenberg, T., Jansen, H., Legtenberg, R. and Elwenspoek, M., "Stiction in Surface Micromachining," *J. Micromech. Microeng*., Vol. 6, No. 4, pp. 385–397 (1996). doi: 10.1088/0960-1317/6/4/005

[8] Wang, H. J., Tsai, H. C., Chen, H. K. and Shing, T. K., "Capillary of Rectangular Micro Grooves and Their Applications to Heat Pipes," *Tamkang Journal of Science and Engineering*, Vol. 8, No. 3, pp. 249–255 (2005). doi: 10.6180/jase.2005.8.3.12

[9] Yang, L. J. and Liu, K. C., "Surface Tension-Driven Micro Valves with Large Rotating Stroke," *Tamkang Journal of Science and Engineering*, Vol. 10, No. 2, pp. 141–146 (2007). doi: 10.6180/jase.2007.10.2.08

[10] Mastrangelo, C. H. and Hsu, C. H., "Mechanical Stability and Adhesion of Microstructures under Capillary Forces- Part I: Basic Theory," *Journal of Microelectromechanical Systems*, Vol. 2, No. 1, pp. 33–43 (1993). doi: 10.1109/84.232593

[11] Mastrangelo, C. H. and Hsu, C. H., "A Simple Experimental Technique for the Measurement of the Work of Adhesion of Microstructures," *Technical Digest - IEEE Solid-State Sensor and Actuator Workshop*, pp. 208–212 (1992). doi: 10.1109/SOLSEN.1992.228291

[12] Mastrangelo, C. H. and Hsu, C. H., "Mechanical Stability and Adhesion of Microstructures under Capillary Forces- Part II: Experiments," *Journal of Microelectromechanical Systems*, Vol. 2, No. 1, pp. 44–55 (1993). doi: 10.1109/84.232594

[13] Fortes, M. A., "Axisymmetric Liquid Bridges between Parallel Plates," *J. Colloid and Interface Science*, Vol. 88, No. 2, pp. 338–351 (1982). doi: 10.1016/0021-9797(82)90263-6

[14] Gere, J. M. and Timoshenko, S. P., *Mechanics of Materials*, 2nd ed., Brooks/Cole Engineering Division, Monterey, California, p. 736 (1984). doi: 10.1115/1.3269380

[15] Yang, L. J., Jan, D. L. and Lin, W. C., "Steel-Based

Bionic Actuators for Flapping Micro-Air-Vehicles," *Micro and Nano Letters*, Vol. 8, No. 10, pp. 686–690 (2013). doi: 10.1049/mnl.2013.0316

[16] Bico, J., Roman, B., Moulin, L. and Boudaoud, A., "Elastocapillary Coalescence in Wet Hair," *Nature*, Vol. 432, p. 690 (2004). doi: 10.1038/432690a

Manuscript Received: Apr. 7, 2014
Accepted: Jul. 31, 2014